Molecular Biology of the Cell
Vol. 11, 635–645, February 2000

The Role of the Tethering Proteins p115 and GM130 in Transport through the Golgi Apparatus In Vivo

Joachim Seemann,*† Eija Jämsä Jokitalo,*‡ and Graham Warren§

*Cell Biology Laboratory, Imperial Cancer Research Fund, London WC2A 3PX, United Kingdom; and §Department of Cell Biology, Yale University School of Medicine, New Haven, Connecticut 06520-8002

Submitted September 29, 1999; Revised November 11, 1999; Accepted November 15, 1999
Monitoring Editor: Peter Walter

Biochemical data have shown that COPI-coated vesicles are tethered to Golgi membranes by a complex of at least three proteins: p115, giantin, and GM130. p115 binds to giantin on the vesicles and to GM130 on the membrane. We now examine the function of this tethering complex in vivo. Microinjection of an N-terminal peptide of GM130 or overexpression of GM130 lacking this N-terminal peptide inhibits the binding of p115 to Golgi membranes. Electron microscopic analysis of single microinjected cells shows that the number of COP-sized transport vesicles in the Golgi region increases substantially, suggesting that transport vesicles continue to bud but are less able to fuse. This was corroborated by quantitative immunofluorescence analysis, which showed that the intracellular transport of the VSV-G protein was significantly inhibited. Together, these data suggest that this tethering complex increases the efficiency with which transport vesicles fuse with their target membrane. They also provide support for a model of mitotic Golgi fragmentation in which the tethering complex is disrupted by mitotic phosphorylation of GM130.

INTRODUCTION

Transport along the secretory pathway is mediated by vesicles that bud from one membrane compartment and fuse with the next in the pathway (Rothman, 1994). Two types of coated vesicles, COPI and COPII, have been implicated in the early part of this pathway. COPII vesicles bud exclusively from the endoplasmic reticulum (ER), carrying cargo from the ER to the Golgi apparatus (Barlowe *et al.*, 1994; Barlowe, 1998), whereas COPI vesicles have been implicated in anterograde transport of cargo molecules through the Golgi stacks (Rothman and Wieland, 1996; Orci *et al.*, 1997) and/or retrograde recycling of molecules back to the ER (Letourneur *et al.*, 1994; Pelham, 1998).

After budding, both types of vesicles uncoat in preparation for fusion with their target membrane (Gaynor *et al.*, 1998; Lowe and Kreis, 1998). The SNARE hypothesis has provided a mechanism to explain both the specificity of fusion (Söllner *et al.*, 1993) and even the fusion process itself (Weber *et al.*, 1998). It postulates that vesicle targeting is mediated by soluble *N*-ethylmaleimide–sensitive fusion protein receptors (SNAREs) (Söllner *et al.*, 1993), a SNARE on the vesicle (v-SNARE) docking with a SNARE on the target membrane. Docking is crucial for membrane fusion (Weis and Scheller, 1998; Owen and Schiavo, 1999), although other factors may refine the specificity and may be needed for the actual fusion event itself.

SNARE-mediated docking is preceded by the tethering of vesicles to their target membrane (Pfeffer, 1996, 1999). Tethers were first described for ER-to-Golgi (Nakajima *et al.*, 1991; Lupashin *et al.*, 1996; Cao *et al.*, 1998) and intra-Golgi (Waters *et al.*, 1992) transport, but now they include endosome–endosome fusion (Christoforidis *et al.*, 1999; McBride *et al.*, 1999), homotypic fusion of vacuoles (Ungermann *et al.*, 1998), as well as fusion of secretory vesicles with the plasma membrane (Terbush *et al.*, 1996; Guo *et al.*, 1999; Hsu *et al.*, 1999). In each case, the tethering complex is regulated by small GTPases of the Ypt/rab family of proteins (Pfeffer, 1999). In many cases, the tethers are thought to be long fibrous proteins with extensive regions of predicted coiled coil (Nakajima *et al.*, 1991; Mu *et al.*, 1995; Sapperstein *et al.*, 1995) that can be visualized by electron microscopy (Weidman *et al.*, 1993; Sapperstein *et al.*, 1995; Yamakawa *et al.*, 1996; Orci *et al.*, 1998).

One of the best characterized tethering factors is p115 and its yeast homologue Uso1p. p115 was isolated as a factor required for intra-Golgi transport (Waters *et al.*, 1992) and as a component of transcytotic vesicles (Sztul *et al.*, 1993). Uso1p is required for the initial docking event of COPII vesicles to the Golgi apparatus, a process that depends on Ypt1 but is independent of SNARE proteins (Cao *et al.*, 1998).

The Golgi membrane binding sites for the mammalian homologue p115 have been identified. p115 binds to GM130, which is the receptor on the Golgi complex (Nakamura *et al.*, 1997), and to giantin on COPI vesicles during tethering to

‡ Present address: Institute of Biotechnology, Electron Microscopy Unit, University of Helsinki, Viikinkaari 9, 00014 Helsinki, Finland.
† Corresponding author. E-mail address: joachim.seemann@yale.edu.

Golgi membranes (Sönnichsen *et al.*, 1998). It has also been shown that p115 functions in stacking of cisternae during the postmitotic formation of Golgi stacks in vitro (Shorter and Warren, 1999). The binding site for p115 is located in the N-terminal domain of GM130, because a peptide corresponding to the 73 N-terminal amino acids competes for binding (Nakamura *et al.*, 1997; Sönnichsen *et al.*, 1998). Furthermore, a mutant of GM130 lacking the N-terminal 75 residues fails to bind p115 in vitro and in vivo (Nakamura *et al.*, 1997).

The p115/GM130 tethering complex is regulated by phosphorylation during mitosis (Nakamura *et al.*, 1997). At the onset of mitosis, GM130 is phosphorylated (Lowe *et al.*, 1998b), and this inhibits the binding of p115 to the Golgi apparatus in vitro (Levine *et al.*, 1996) and in vivo (Shima *et al.*, 1997). This is thought to prevent tethering of COPI vesicles and, as a consequence, inhibit transport through the Golgi apparatus during mitosis (Lowe *et al.*, 1998a). Continuous budding without fusion would also convert cisternae to vesicles, which would help explain the observed fragmentation of the Golgi apparatus into clusters of vesicles during the early phases of mitosis (Cabrera-Poch *et al.*, 1998).

However, it has been difficult to provide evidence for this hypothesis in vivo. Manipulating mitotic cells is still technically difficult, so we have opted to disrupt the p115/GM130 tethering complex in interphase cells by microinjecting GM130 peptides or expressing GM130 constructs. The results show clearly that disrupting these complexes inhibits transport and has the expected effect on the accumulation of transport-sized vesicles.

MATERIALS AND METHODS

Cell Culture

Normal rat kidney (NRK) cells were grown in DMEM (Life Technologies-BRL, Gaithersburg, MD) supplemented with 10% FCS at 37°C and 10% CO_2 in a humidified atmosphere. For microinjection experiments and for immunofluorescence microscopy, NRK cells were grown on glass coverslips.

Antibodies and Plasmids

The following antibodies were used: mAb P5D4 against the C-terminal domain of VSV-G (Kreis and Lodish, 1986), mAb 4H1 against p115 (Waters *et al.*, 1992), mAb 2C10 and affinity-purified rabbit antibody NN16 against GM130 (Nakamura *et al.*, 1995), mAb GTL2 against rat β-1,4 galactosyltransferase (Kawano *et al.*, 1994), affinity-purified rabbit antibody against the lumenal domain of VSV-G (K. Simons, EMBL, Heidelberg, Germany), rabbit antibody against mammalian Sec13p (Tang *et al.*, 1997), and affinity-purified rabbit antibody against β-COP (Pepperkok *et al.*, 1993). Rhodamine- and FITC-coupled secondary antibodies were obtained from Biosource (Camarillo, CA), and Texas red–conjugated secondary antibodies were obtained from Molecular Probes (Eugene, OR). The full-length GM130 (fl GM130) construct in pCMUIV has been described (Nakamura *et al.*, 1997). The Δ63 GM130 construct was generated by PCR, cloned into pCMUIV, and verified by sequencing. All plasmids were purified on columns (Qiagen, Hilden, Germany) according to the manufacturer's protocol.

Microinjection

Capillary microinjection into NRK cells was performed with the use of a semiautomatic system consisting of the Transjector 55246 and the Micromanipulator 5171 (Eppendorf, Hamburg, Germany) connected to an inverted Axiovert-10 microscope (Carl Zeiss, Oberkochen, Germany). Needles were pulled from 1.2-mm-diameter glass capillaries (Clark Electromedical Instruments, Reading, UK) with the use of a P-97 needle puller (Sutter Instruments, Novato, CA). The N73 peptide or control peptide (p115.4, corresponding to amino acids 907–919 of p115) (Nakamura *et al.*, 1997) was injected into the cytoplasm at 5 or 1 mg/ml. The peptides were mixed with 2 mg/ml cascade blue–conjugated BSA (Molecular Probes) as an injection marker for immunofluorescence microscopy or with protein A coupled with 10-nm gold (Department of Cell Biology, Utrecht School of Medicine, Utrecht, Netherlands) as an injection marker for electron microscopy, respectively. For transient expressions, plasmid DNA was injected into nuclei at a concentration of 0.1 mg/ml.

Immunofluorescence and Quantitation of VSV-G Protein Transport

For analysis of transport of the temperature-sensitive mutant of the VSV-G protein (ts-O45-G), NRK cell nuclei were microinjected with a mixture of plasmids encoding the cDNA of VSV-G and fl GM130 or Δ63 GM130. After injection, the cells were incubated for 30 min at 37°C and then shifted to 39.5°C for 6.5 h. After 30 min of incubation at 4°C to enhance the folding of the ts-O45-G (Scales *et al.*, 1997), cycloheximide was added to a final concentration of 0.1 mg/ml. The transport of the VSV-G protein was induced at 31.5°C for 30 or 60 min. For staining the VSV-G protein at the plasma membrane, cells were fixed for 15 min with 4% paraformaldehyde in PBS and quenched for 15 min in 50 mM NH_4Cl in PBS. After washing in PBS, the cells were incubated with rabbit antibodies specific for the lumenal domain of the VSV-G protein. The cells were washed again, and bound antibodies were fixed for 15 min in 4% paraformaldehyde in PBS followed by incubation for 15 min in 50 mM NH_4Cl in PBS. Subsequently, the cells were permeabilized for 4 min in 0.1% Triton X-100 in PBS, followed by incubation with the mAb P5D4 against the VSV-G protein to detect the total pool of the VSV-G. After washing in PBS, the cells were incubated with two secondary antibodies (FITC anti-mouse and rhodamine anti-rabbit antibodies), washed again, and mounted in Moviol 4-88 (Harco, Harlow, UK). Fluorescence analysis was performed with the use of a Zeiss Axiovert 135TV inverted microscope (Carl Zeiss), and images were captured on a cooled charge-coupled device camera (1035 × 1317 pixels; Princeton Instruments, Trenton, NJ). Images were analyzed and quantified with the use of the software package IP Lab Spectrum version 3.1 (Signals Analytics, Vienna, VA) essentially as described (Pepperkok *et al.*, 1993). For all quantitations, images were captured at the same exposure times and settings of the charge-coupled device camera. Background fluorescence was measured on cells from the same coverslip, which did not express ts-O45-G, and was subtracted from the signal of cells positive for VSV-G labeling. After the area (A) of the cell was defined manually, the mean fluorescence (I) and the area of the cell was measured with the use of IP Lab Spectrum. The integrated optical density (IOD) was then determined by the formula $IOD = A \times I$, according to Pepperkok *et al.* (1993). To correct for different expression levels, the ratio of the surface to total IOD of VSV-G was determined for each cell analyzed and expressed as the mean ± SD for at least 20 cells in two independent experiments.

Electron Microscopy

After microinjection of peptide or cDNA, cells were incubated at 37°C for 1 or 3 h and fixed with 2% glutaraldehyde (electron microscopy grade; Fluka, Buchs, Switzerland) in 0.1 M Na cacodylate buffer, pH 7.4, for 30 min at room temperature. Fixed cells on coverslips were treated with reduced osmium tetroxide and dehydrated with a graded series of ethanol, and a plastic capsule filled with Epon 812 (Taab Laboratories, Reading, UK) was placed upside-down on top of the coverslip. After polymerization, the glass cov-

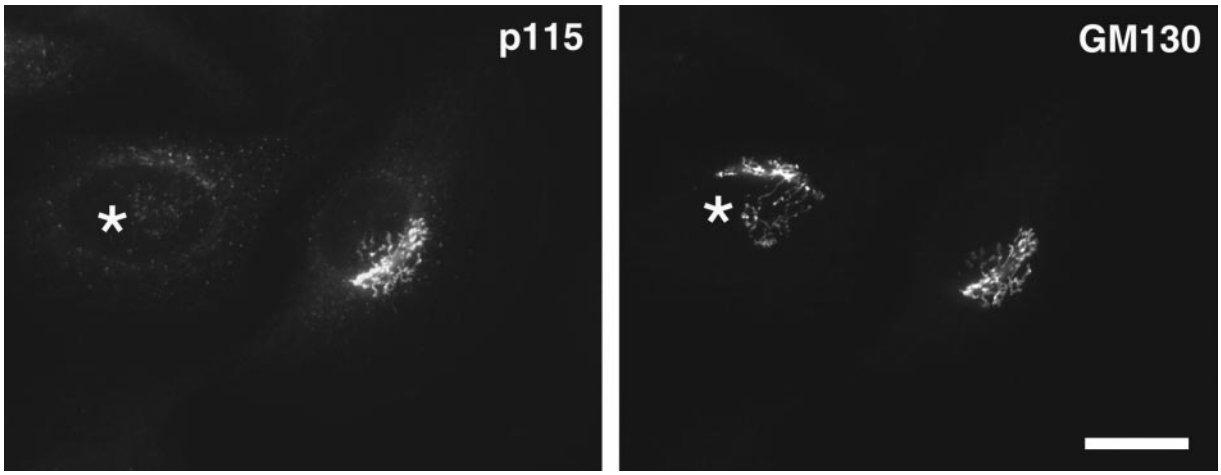

Figure 1. N73pep inhibits p115 binding to the Golgi apparatus. The N-terminal peptide of GM130 (N73pep) was microinjected together with cascade blue–conjugated BSA as an injection marker into the cytoplasm of NRK cells. After 1 h, the cells were fixed, permeabilized, and double labeled with a mAb to p115 and polyclonal antibodies to GM130 followed by fluorescently conjugated secondary antibodies (Texas red anti-mouse and FITC anti-rabbit antibodies). The injected cell is marked by an asterisk. Bar, 15 μm.

erslips were removed by dipping them in liquid nitrogen. Sections parallel to the coverslip were cut with the use of an ultramicrotome 2E (Reichert–Jung, Vienna, Austria) set to 65 nm, picked up on a copper grid, stained with 2% uranyl acetate and lead citrate, and viewed with the use of an electron microscope (CM10, Philips Electronics, Mahwah, NJ) at 60 kV.

Stereology

The Golgi area was defined by the boundary enclosing the Golgi stacks, tubules, and tubulo-reticular networks and all vesicles that were within 70 nm of these membranes. The area was estimated by the point hit method with a 5-mm square grid laid over pictures printed at a final magnification of ×29,900. Small vesicles, defined as circular profiles with a diameter of 50–80 nm, with or without a coat, and falling inside the Golgi area, were then counted, and results are expressed as number of vesicles per square micrometer of Golgi area. Quantitation was performed from two experiments on 18 microinjected cells and 8 uninjected control cells from the same section.

For estimation of the diameter of these vesicles, pictures were scanned and the diameter was measured with the use of the software package IP Lab Spectrum version 3.1 (Signals Analytics). Measurements were done on 100–150 vesicles at a final magnification of ×120,000.

When studying the effect of Δ63 GM130 expression on Golgi morphology, membrane profiles in the Golgi area were divided into four categories: cisternae, tubules, vesicles, and others. Cisternae were defined, as described previously (Misteli and Warren, 1994), as membrane profiles with a length more than four times their width, the width being no more than 80 nm; tubules had a length less than four times their maximal width; vesicles had round profiles with a diameter of 50–80 nm; and others had mainly round profiles with a diameter of 100–200 nm. A 4-mm line grid was laid over pictures printed at ×52,000 final magnification, and the number of intersections of each membrane structure with lines was counted. The relative proportion of each category of membranes was then calculated as $N_{\text{intersections in category}}/N_{\text{total intersections}}$ and expressed as a percentage of the total membrane. These results were compared with the results obtained from cells overexpressing the fl GM130. A total of 10,140 intersections from 16 cells expressing Δ63 GM130 and 5,200 intersections from 8 cells expressing the full-length protein from two experiments were counted.

RESULTS

Microinjection of the N-Terminal Peptide of GM130 Leads to Accumulation of Vesicles in the Golgi Region

p115 is localized to the Golgi apparatus (Waters *et al.*, 1992; Sapperstein *et al.*, 1995) and peripheral punctuate structures corresponding to vesicular tubular clusters (VTCs) that are involved in ER-to-Golgi transport (Nelson *et al.*, 1998). We have shown previously that p115 is targeted to the Golgi complex by binding to the *cis*-Golgi matrix protein GM130 (Nakamura *et al.*, 1997). The binding site for p115 in GM130 is localized in the N-terminal 73 amino acids, and a synthetic peptide comprising the N-terminal 73 residues of GM130 (N73pep) is sufficient to compete for the binding of p115 to GM130 on the Golgi complex (Nakamura *et al.*, 1997; Sönnichsen *et al.*, 1998). To analyze the effect in vivo, we microinjected the synthetic peptide N73pep (Nakamura *et al.*, 1997) into NRK cells. One hour after injection, the cells were fixed and subjected to double immunofluorescence microscopy with the use of antibodies against p115 (mAb 4H1) and GM130 (NN16) followed by fluorescently conjugated secondary antibodies. Under these conditions, the level of p115 on the Golgi apparatus was reduced significantly and p115 was redistributed to the cytosol in peptide-injected cells but not in uninjected cells (Figure 1, left). However, the injected peptide had no effect on binding of p115 to the peripheral punctuate structures representing VTCs. Because GM130 is not required for the binding of p115 to VTCs (Nelson *et al.*, 1998), the microinjected peptide had a specific effect on the localization of p115 to the Golgi apparatus and not to other membranes.

Furthermore, the localization of GM130 in injected cells was not changed, as shown by double staining with anti-

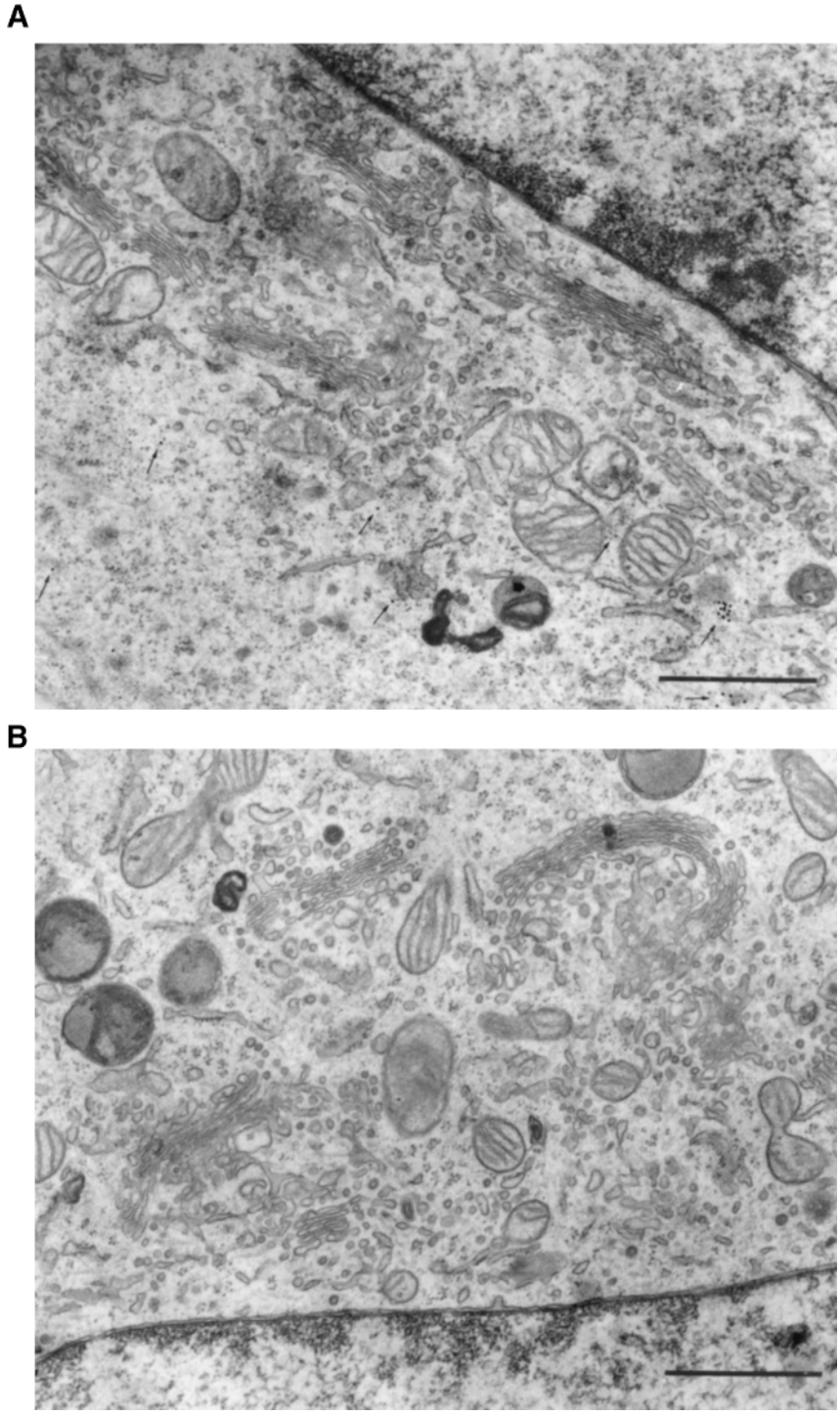

Figure 2. Ultrastructure of NRK cells microinjected with N73pep. The cytoplasm of NRK cells was microinjected with the N73pep mixed with 10-nm protein A–gold as an injection marker (top; gold particles indicated by arrows). Cells were fixed after 1 h of incubation and processed for electron microscopy. In microinjected cells (top), the number of vesicles in the Golgi region was increased (see Table 1 for quantitations) compared with uninjected cells in the same section (bottom). Bar, 1 μm.

bodies against GM130 (Figure 1, right). This result shows that the effect on p115 was not the consequence of a redistribution of its receptor GM130. The microinjected peptide likely competes with GM130 for p115 binding to the *cis*-Golgi membranes.

We further analyzed the effect of relocalization of p115 by electron microscopy. NRK cells were microinjected with the N73pep or a control peptide. The peptides were mixed with protein A coupled to 10-nm gold particles as an injection marker. Cells were fixed 1 h after microinjection and pro-

Table 1. Reduced p115 binding to the Golgi apparatus leads to an accumulation of vesicles in the Golgi region

Injection	Incubation time (h)	Number of vesicles per square meter of Golgi area		Increase in vesicle number (%)
		Injected cells	Uninjected cells	
N73pep	1	31 ± 4.2	23 ± 3.4	35
N73pep	3	31 ± 5.4	22 ± 5.8	41
Control peptide	1	28 ± 5.1	26 ± 4.2	8
Protein A–gold	1	35 ± 5.2	32 ± 2.6	9

NRK cells were microinjected with N73pep or a control peptide (p115.4, residues 907–919 of p115) together with 10-nm protein A–gold as a marker to identify injected cells. The cells were incubated for 1 or 3 h, fixed, and processed for electron microscopy. The number of vesicles per square meter of Golgi area was determined for injected and uninjected cells as described in MATERIALS AND METHODS.

cessed for Epon embedding. Microinjected cells were identified in thin sections by the gold particles in the cytoplasm (Figure 2, top, arrows). The morphology of the Golgi apparatus was very similar in injected and uninjected cells from the same section (Figure 2, bottom). However, quantitation of the number of vesicles per square micrometer of the Golgi area revealed an increase of 35% in cells injected with the N73pep compared with uninjected cells in the same section (Table 1). A similar result was obtained when the cells were fixed 3 h after the peptide injection, showing that steady-state conditions were reached after 1 h. To exclude the possibility of a nonspecific effect caused by the microinjection procedure, we measured the increase of vesicles in cells injected with a control peptide (p115.4, corresponding to amino acids 907–919 of p115) together with the injection marker or the injection marker alone. The number of vesicles increased by 8 and 9%, respectively, showing that the increase in the number of vesicles in the Golgi area is the consequence of redistributing p115 by microinjected N73pep.

Furthermore, the vesicles that accumulated appeared to be very uniform in size and shape. In N73pep-injected cells, the diameter of the vesicular profiles in the Golgi area (58 ± 5 nm) was indistinguishable from that of uninjected cells (59 ± 5 nm). This diameter is also in the size range of coated COPI and COPII vesicles, which have diameters of 60–75 nm (Orci *et al.*, 1986; Malhotra *et al.*, 1989; Oprins *et al.*, 1993; Barlowe *et al.*, 1994), and uncoated COPI vesicles, which have diameters of 50–57 nm (Lucocq *et al.*, 1989; Oprins *et al.*, 1993; Misteli and Warren, 1994). This finding suggests that the vesicles that accumulate are transport vesicles.

Truncated GM130 Replaces Endogenous GM130 and Prevents p115 Binding

Because the inhibition of p115 binding to Golgi membranes caused an accumulation of vesicles of the size of transport vesicles, we investigated the transport of newly synthesized protein. NRK cells were microinjected with the N73pep and, after 60 min of incubation, the cells were injected a second time with the cDNA encoding the plasma membrane marker CD8. The transport of newly synthesized CD8 was then analyzed (Shima *et al.*, 1998). Unfortunately, owing to the variation in the amount of material microinjected and the variable expression levels of the CD8 caused by injecting the cells twice, surface fluorescence of CD8 was too variable and quantitation of the rate of transport was not reliable. To overcome these technical difficulties, a different approach was used. We previously showed that removal of the N-terminal domain of GM130 completely abolished the binding of p115 but had no effect on the targeting of GM130 to the Golgi apparatus (Nakamura *et al.*, 1997). After overexpression of the Δ63 GM130 mutant by microinjection of the plasmid, endogenous GM130 was not detectable with the use of an antibody specific for the N-terminal domain of GM130, showing that the mutant had replaced the endogenous GM130 on the Golgi membranes (Figure 3, A and B). Under these conditions, p115 was no longer detectable on the Golgi apparatus (Figure 3, C and D). This effect was not due to overexpression, because expression of fl GM130 had no effect on the targeting of p115 to the Golgi complex (our unpublished results). Furthermore, overexpression did not interfere significantly with the morphology of the Golgi apparatus, because the localization of the Golgi resident enzyme β-1,4 galactosyltransferase was not affected (Figure 3, E and F).

Disruption of the p115/GM130 Complex Inhibits Transport of VSV-G

To analyze the effect of disrupting the p115/GM130 complex on the transport through the Golgi apparatus, we used ts-O45-G as a cargo molecule. It misfolds at 39.5°C and fails to exit the ER. After shifting to the permissive temperature (31.5°C), ts-O45-G folds rapidly and is transported from the ER through the Golgi apparatus to the plasma membrane (Bergmann and Singer, 1983). For the analysis of transport, the cDNA of VSV-G was mixed and coinjected together with that for Δ63 GM130. We chose this approach rather than double injection to ensure expression of both plasmids at the same time at similar levels in different injected cells. During incubation at 39.5°C, both proteins, GM130 and VSV-G, were expressed. However, because ts-O45-G is a temperature-sensitive folding mutant of VSV-G, it failed to fold properly and was retained in the ER, whereas GM130 was targeted correctly to the Golgi apparatus, where it replaced the endogenous molecule. After 6.5 h of incubation, which was sufficient time to accumulate enough VSV-G in the ER and to replace the endogenous GM130 on the Golgi apparatus, cycloheximide was added and the cells were shifted to the permissive temperature (31.5°C), which allowed transport of the ts-O45-G that had been synthesized.

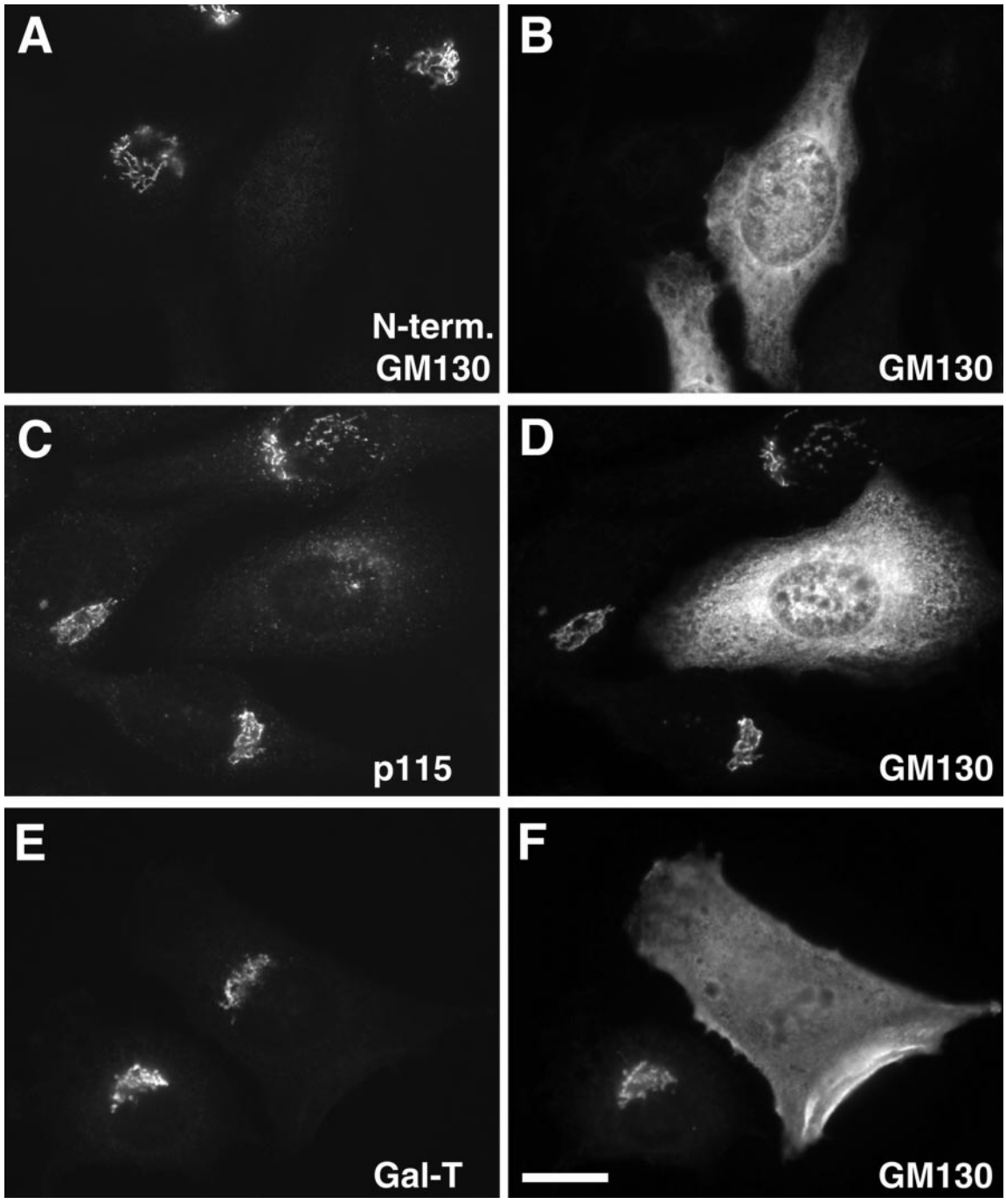

Figure 3. Truncated GM130 replaces endogenous GM130 on the Golgi apparatus and prevents p115 binding. The N-terminally truncated Δ63 GM130 was transiently expressed in NRK cells by microinjection of the encoding plasmid. Cells were fixed and permeabilized by treatment with cold methanol and double labeled with monoclonal (B) or polyclonal (D and F) antibodies to GM130 and rabbit antibodies to the N-terminal domain of GM130 (A), a mAb to p115 (C), or a mAb to β-1,4 galactosyltransferase (GalT; E). Secondary antibodies were coupled to FITC (anti rabbit) or Texas red (anti mouse). Bar, 15 μm.

After 60 min, the cells were fixed and VSV-G on the plasma membrane was stained with polyclonal antibodies specific for the extracellular domain of the G protein. After permeabilization, the mAb P5D4 against the cytoplasmic domain of VSV-G was used to detect the total pool of VSV-G. This allowed us to correct for different expression levels when comparing transport in different cells. As shown in Figure 4, at similar levels of total

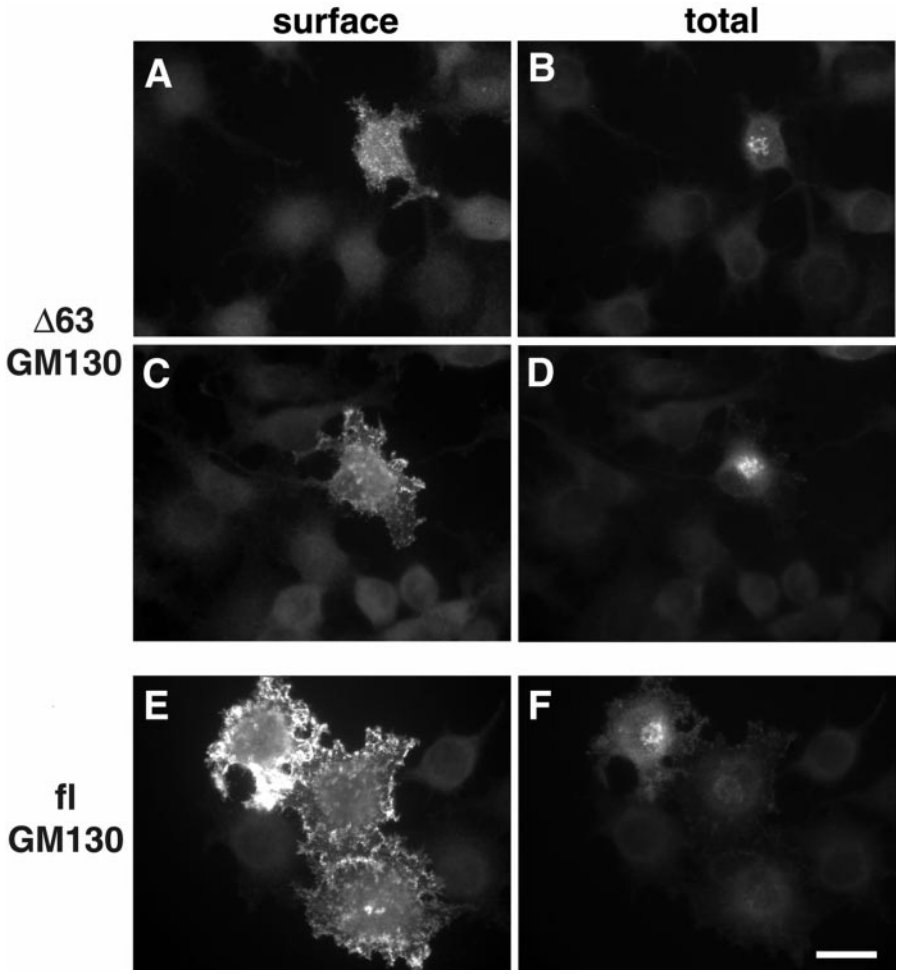

Figure 4. Inhibition of p115 binding to the Golgi apparatus inhibits transport of VSV-G to the plasma membrane. NRK cells were microinjected with a mixture of plasmids encoding Δ63 GM130 or fl GM130 and VSV-G (ts-O45-G). After expression of the proteins for 6.5 h at 39.5°C, the temperature was shifted to 31°C for 60 min in the presence of cycloheximide. After fixation with paraformaldehyde, VSV-G on the cell surface was visualized with rabbit antibodies to the lumenal domain of the VSV-G protein (A, C, and E). The cells were then permeabilized and labeled with a mAb to the cytoplasmic domain (B, D, and F) followed by secondary antibodies coupled to rhodamine (anti rabbit) and FITC (anti mouse). After 60 min at the permissive temperature, surface fluorescence was lower in cells expressing Δ63 GM130 (A–D) than in cells expressing fl GM130 (E and F) at similar expression levels. Note that the surface fluorescence is greater than the total fluorescence because polyclonal antibodies were used to detect the former and mAbs were used to detect the latter. Bar, 20 μm.

VSV-G protein, cells expressing the Δ63 GM130 mutant had lower levels of surface G protein than those expressing fl GM130. Note that the surface fluorescence was brighter than the total fluorescence because polyclonal antibodies were used to detect the former and mAbs were used to detect the latter. This observation indicates that transport of VSV-G to the plasma membrane is significantly inhibited if the binding of p115 to the Golgi membranes is blocked.

To quantify the inhibition of transport, NRK cells expressing VSV-G and Δ63 GM130 or fl GM130 were shifted for 30 or 60 min to the permissive temperature and double labeled for VSV-G on the cell surface and in the cell, as described above. The amounts of VSV-G reaching the plasma membrane and the total pool of the VSV-G protein were quantified by immunofluorescence, and the ratio of the two signals was determined for each cell analyzed. After 30 min of transport, the rate of VSV-G appearance on the cell surface was inhibited by 65% in cells expressing Δ63 GM130 compared with cells expressing fl GM130. A similar result was obtained when the cells were shifted to the permissive temperature for 60 min. In this case, transport of VSV-G to the cell surface was inhibited by 62% (Figure 5). This inhibition confirmed that binding of p115 to the Golgi apparatus is required for efficient transport of VSV-G to the plasma membrane.

Inhibition of p115 Binding to the Golgi Apparatus Leads to an Increase in Golgi Vesicles

Expression of GM130 lacking the N-terminal domain should lead to an accumulation of vesicles, as observed after injection of the N73pep. To analyze this, the Δ63 GM130 mutant or fl GM130 was transiently expressed by microinjection of the cDNA into the nuclei of NRK cells. Protein A–gold was coinjected as an injection marker to identify microinjected cells in the thin sections. After 3 h of expression, endogenous GM130 was replaced by the Δ63 GM130 mutant on the Golgi apparatus and p115 was no longer detectable on the Golgi, as monitored by immunofluorescence. The cells were fixed and processed for electron microscopy. In cells expressing fl GM130, the morphology of the Golgi apparatus (Figure 6) was essentially the same as in uninjected cells (Figure 2) or control cells injected with the injection marker, protein A–gold, alone (data not shown). However, expression of the Δ63 GM130 mutant changed the morphology of the Golgi complex in a dramatic manner. In these cells, the number of

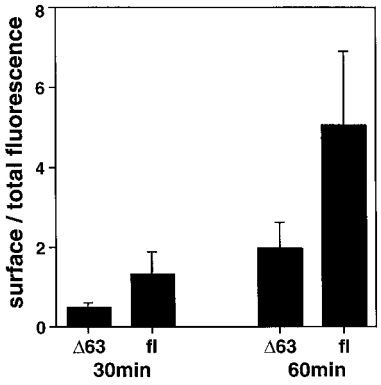

Figure 5. Quantitation of the appearance of VSV-G on the cell surface. NRK cells expressing VSV-G (ts-O45-G) and Δ63 GM130 or fl GM130 were shifted to the permissive temperature for 30 or 60 min and double labeled for VSV-G on the cell surface and in intracellular structures, as described in Figure 4. Surface and internal fluorescence of the VSV-G protein were quantified, and the ratio of the two signals was determined for each cell analyzed and expressed as the mean ± SD. Note that the ratio of surface fluorescence to total fluorescence is >1 because polyclonal antibodies were used to detect the former and mAbs were used to detect the latter.

vesicles located in the Golgi area increased dramatically, whereas the length of the cisternae decreased (Figure 6). Furthermore, the vesicular structures were restricted and concentrated in the Golgi area. Stereological analysis revealed that the amount of Golgi membrane present in vesicles and tubules increased in cells expressing the mutant lacking the N-terminal domain. The percentage of Golgi membranes in vesicles increased by 26%, and tubular structures increased by 11% (Table 2). This increase in tubular and vesicular structures was matched by a decrease of 38% in membrane present in cisternae (Table 2), suggesting conversion of cisternae into vesicular and tubular structures.

DISCUSSION

In this study, we have used an in vivo approach to characterize the interaction of p115 with GM130. The disruption of this tethering complex led to an increase in transport vesicles and an inhibition of transport. Our evidence suggests that tethering is required for efficient transport of cargo through the Golgi apparatus.

The tethering complex was disrupted in two ways. First, by microinjection of the N-terminal domain of GM130, which is known to inhibit the binding of p115 to GM130 in vitro and in vivo (Sönnichsen *et al.*, 1996; Nakamura *et al.*, 1997; Shorter and Warren, 1999). Our ultrastructural analysis of the microinjected cells showed that inhibition of binding of p115 to the Golgi apparatus led to a 35–40% increase in the number of vesicles in the Golgi area.

The second approach was to express a mutant of GM130 lacking the corresponding residues in the N-terminal domain (Nakamura *et al.*, 1997). After replacement of the endogenous GM130 by the mutant protein, we could no longer detect p115 on the Golgi apparatus, and transport of the temperature-sensitive viral glycoprotein ts-O45-G to the plasma membrane was inhibited significantly. Furthermore, ultrastructural analysis showed that the number of vesicles in the Golgi area increased by almost 100%.

Although both methods led to an accumulation of vesicles, the number was much higher in the experiments with the Δ63 GM130 mutant. This is perhaps due to the different means of displacing p115 from the Golgi apparatus. The peptide only competes with GM130 for p115, so some p115 might remain on the Golgi. In contrast, the mutant GM130 might replace so much of the endogenous GM130 that no binding site for p115 remains, which in turn could lead to the accumulation of more vesicles. It is also possible that removal of the p115-binding site on the Golgi apparatus might interfere with Golgi structure. Recent experiments have proposed a function for p115 in stacking the rims of Golgi cisternae (Shorter and Warren, 1999). The removal of the p115-binding site might destabilize the rims of the cisternae and thus facilitate the consumption of the membrane by continued budding of vesicles.

The vesicles that accumulated under both conditions appeared to be uncoated, and several lines of evidence suggest that they are COPI transport vesicles. First, they are the same size. COPI vesicles have a diameter of 60–70 nm (taking into account the thickness of the coat [Oprins *et al.*, 1993; Kreis *et al.*, 1995]), and the vesicles that accumulated had a diameter of 59 ± 5 nm. Second, they were the same size as mitotic Golgi vesicles (57 nm; Lucocq *et al.*, 1989), which are thought to be the product of continued budding of COPI vesicles from Golgi cisternal rims (Lucocq *et al.*, 1989; Misteli and Warren, 1994). Third, the loss of cisternal membrane after expressing Δ63 GM130 was matched by an increase in vesicles and tubules, suggesting again that they are the product of COPI vesicle budding. Fourth, they accumulate in the Golgi region, which is where COPI vesicles are mostly located (Duden *et al.*, 1991). It seems unlikely that they are COPII vesicles because these are found mostly in the cell periphery in animal cells (Tang *et al.*, 1997; Pepperkok *et al.*, 1998). Staining for COPI (β-COP) and COPII (Sec13p) components confirmed that their overall distribution was not changed by disruption of the tethering complex (our unpublished results). Nevertheless, it is possible that some of the effects on transport could be explained by an inhibition of ER-to-Golgi transport. In yeast, it is clear that COPII vesicles are tethered to Golgi membranes and that they use the yeast homologue of p115, Uso1p. What has still to be investigated is whether it uses a GM130 homologue as a tethering partner.

The partial inhibition of G protein transport can most readily be explained as a shift in the steady-state concentration of intracellular G protein. Disrupting the tethers decreases the efficiency with which the vesicles can fuse with their target membrane, so transport slows down. As the vesicles accumulate, the number compensates for the lack of tethering, and transport speeds up again. It should even reach the original level, the only difference being that each molecule should take, on average, longer to reach the cell surface, which in turn means that the intracellular pool of G protein will be larger than before the treatment. This interpretation is consistent with our data showing a decrease in the ratio of surface to total fluorescence when the mutant GM130 is expressed. This translates into an increase in the intracellular pool of G protein. It is also consistent with the increase in vesicles after microinjection of the N-terminal

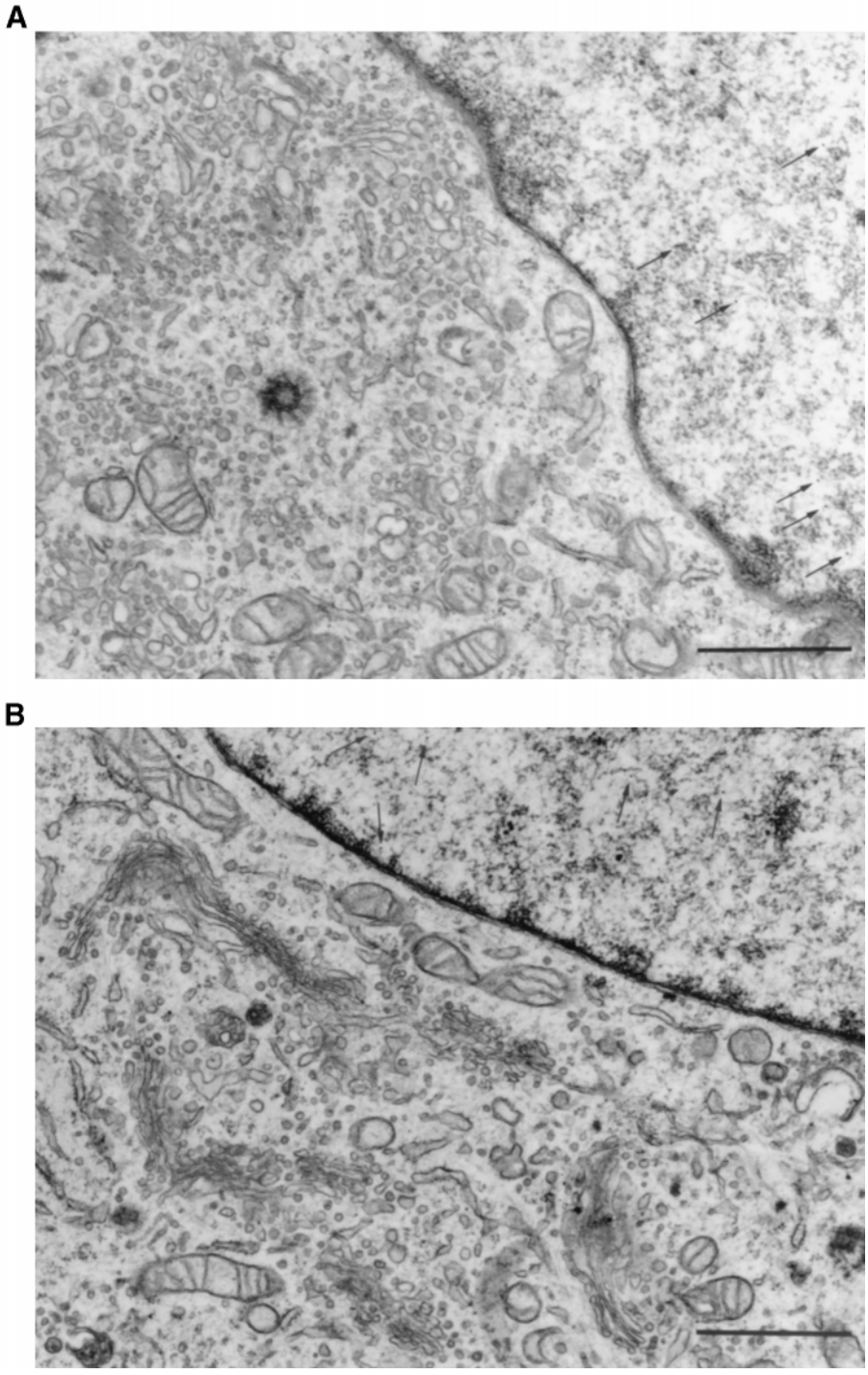

Figure 6. Increase in Golgi vesicles after replacing endogenous GM130 by the Δ63 GM130 mutant lacking the p115-binding site. Δ63 GM130 or fl GM130 was transiently expressed by microinjection of the cDNA into the nuclei of NRK cells. Protein A–gold was coinjected as a marker to identify microinjected cells (gold particles in the nuclei are indicated by arrows). After 3 h of expression, the cells were fixed and processed for electron microscopy. In cells expressing the Δ63 GM130 mutant, the number of vesicles located in the Golgi area increased and the length of the cisternae decreased (top). In contrast, overexpression of fl GM130 (bottom) had no effect on the morphology of the Golgi apparatus (see Figure 2, bottom). See Table 2 for quantitations. Bar, 1 μm.

GM130 peptide. A new steady state was reached after 1 h and was maintained for at least 2 h.

An analogous mechanism has been proposed to explain the suppression of certain mutations in Uso1p. The temperature-sensitive phenotype of uso1-1 mutant yeast cells can be suppressed by overexpression of each of the known ER-to-Golgi v-SNAREs (Sapperstein *et al.*, 1996). This was explained as a mass-action effect in which high levels of v-SNAREs increase the probability of SNARE complex formation and thus facilitate fusion of the membranes in the absence of tethering (Sapperstein *et al.*, 1996). In this case, however, suppression is the consequence of increasing the number of proteins that permit vesicles to dock, rather than the number of vesicles.

Table 2. Inhibition of binding of p115 to GM130 on the Golgi apparatus leads to an increase of membrane in vesicles and a decrease of membrane in cisternae

Membrane in	fl GM130	Δ63 GM130	Difference	Change
Vesicles	27 ± 4.6%	53 ± 7.8%	+26%	+96%
Tubules	14 ± 5.6%	25 ± 7.1%	+11%	+79%
Cisternae	60 ± 3.9%	22 ± 9.3%	−38%	−63%

NRK cell nuclei were microinjected with plasmid DNA encoding full-length GM130 (fl GM130) or a mutant lacking the p115-binding site in the N-terminal domain (Δ63 GM130). After 3 h of expression, the cells were fixed and processed for electron microscopy. The parameters were determined as described in MATERIALS AND METHODS.

The reduced docking efficiency of COPI vesicles was proposed to explain the mitotic fragmentation of the Golgi apparatus (Nakamura *et al.*, 1997; Lowe *et al.*, 1998a,b). Mitotic phosphorylation of GM130 by the CDC2 kinase prevents p115 binding (Lowe *et al.*, 1998b), which is thought to prevent tethering of COPI vesicles and, as a consequence, inhibit transport through the Golgi apparatus. In this model, continuous budding would consume the rims of Golgi cisternae, causing COPI vesicles to accumulate (Lowe *et al.*, 1998a), and help to fragment the Golgi apparatus at the onset of mitosis (Cabrera-Poch *et al.*, 1998). In our experiments, we found a correlation between the loss of cisternal membrane and the increase in the number of transport-sized vesicles. However, in contrast to the mitotic conditions, transport of the cargo protein VSV-G to the plasma membrane still occurred, although at a much slower rate. This suggests that the p115/GM130 tethering complex is not the only part of the fusion cycle that is regulated during mitosis and that other targets need to be examined.

The inhibition of tethering during mitosis might be important for the inheritance process of the Golgi. At the onset of mitosis, the Golgi ribbon fragments into a collection of tubules and vesicles and reforms during cytokinesis in each daughter cell (Lucocq *et al.*, 1987; Warren, 1993). Recent work shows that this is a highly ordered and accurate process (Shima *et al.*, 1997) that is organized by the mitotic spindle (Shima *et al.*, 1998). The inhibition of tethering resulting from the mitotic phosphorylation of GM130 might be important for this process, because the binding of p115 to GM130 could cross-link individual clusters and interfere with the accurate partitioning of the Golgi clusters between the daughter cells. This idea can be tested with the use of mutant GM130s once the technical problems of microinjecting mitotic cells are overcome.

ACKNOWLEDGMENTS

We thank Martin Lowe and David Shima for helpful advice and support. We also thank Martin Lowe, Laurence Pelletier, and James Shorter for critical reading of the manuscript. J.S. was supported by a postdoctoral fellowship from the Deutsche Forschungsgemeinschaft.

REFERENCES

Barlowe, C. (1998). CopII and selective export from the endoplasmic reticulum. Biochim. Biophys. Acta *1404*, 67–76.

Barlowe, C., Orci, L., Yeung, T., Hosobuchi, M., Hamamoto, S., Salama, N., Rexach, M.F., Ravazzola, M., Amherdt, M., and Schekman, R. (1994). COPII: a membrane coat formed by Sec proteins that drive vesicle budding from the endoplasmic reticulum. Cell *77*, 895–907.

Bergmann, J.E., and Singer, S.J. (1983). Immunoelectron microscopic studies of the intracellular transport of the membrane glycoprotein (G) of vesicular stomatitis virus in infected Chinese hamster ovary cells. J. Cell Biol. *97*, 1777–1787.

Cabrera-Poch, N., Pepperkok, R., and Shima, D.T. (1998). Inheritance of the mammalian Golgi apparatus during the cell cycle. Biochim. Biophys. Acta *1404*, 139–151.

Cao, X., Ballew, N., and Barlowe, C. (1998). Initial docking of ER-derived vesicles requires Uso1p and Ypt1p but is independent of SNARE proteins. EMBO J. *17*, 2156–2165.

Christoforidis, S., McBride, H.M., Burgoyne, R.D., and Zerial, M. (1999). The Rab5 effector EEA1 is a core component of endosome docking. Nature *397*, 621–625.

Duden, R., Griffiths, G., Frank, R., Argos, P., and Kreis, T.E. (1991). Beta-COP, a 110 kDa protein associated with nonclathrin-coated vesicles and the Golgi complex, shows homology to beta-adaptin. Cell *64*, 649–665.

Gaynor, E.C., Graham, T.R., and Emr, S.D. (1998). COPI in ER/Golgi and intraGolgi transport: do yeast COPI mutants point the way? Biochim. Biophys. Acta *1404*, 33–51.

Guo, W., Grant, A., and Novick, P. (1999). Exo84p is an exocyst protein essential for secretion. J. Biol. Chem. *274*, 23558–23564.

Hsu, S.C., Hazuka, C.D., Foletti, D.L., and Scheller, R.H. (1999). Targeting vesicles to specific sites on the plasma membrane: the role of the sec6/8 complex. Trends Cell Biol. *9*, 150–153.

Kawano, J., Ide, S., Oinuma, T., and Suganuma, T. (1994). A protein-specific monoclonal antibody to rat liver beta 1→4 galactosyltransferase and its application to immunohistochemistry. J. Histochem. Cytochem. *42*, 363–369.

Kreis, T.E., and Lodish, H.F. (1986). Oligomerization is essential for transport of vesicular stomatitis viral glycoprotein to the cell surface. Cell *46*, 929–937.

Kreis, T.E., Lowe, M., and Pepperkok, R. (1995). COPS regulating membrane traffic. Annu. Rev. Cell Biol. *11*, 677–706.

Letourneur, F., Gaynor, E.C., Hennecke, S., Demolliere, C., Duden, R., Emr, S.D., Riezman, H., and Cosson, P. (1994). Coatomer is essential for retrieval of dilysine-tagged proteins to the endoplasmic reticulum. Cell *79*, 1199–1207.

Levine, T.P., Rabouille, C., Kieckbusch, R.H., and Warren, G. (1996). Binding of the vesicle docking protein p115 to Golgi membranes is inhibited under mitotic conditions. J. Biol. Chem. *271*, 17304–17311.

Lowe, M., and Kreis, T.E. (1998). Regulation of membrane traffic in animal cells by COPI. Biochim. Biophys. Acta *1404*, 53–66.

Lowe, M., Nakamura, N., and Warren, G. (1998a). Golgi division and membrane traffic. Trends Cell Biol. *8*, 40–44.

Lowe, M., Rabouille, C., Nakamura, N., Watson, R., Jackman, M., Jamsa, E., Rahman, D., Pappin, D.J., and Warren, G. (1998b). Cdc2 kinase directly phosphorylates the cis-Golgi matrix protein GM130 and is required for Golgi fragmentation in mitosis. Cell *94*, 783–793.

Lucocq, J.M., Berger, E.G., and Warren, G. (1989). Mitotic Golgi fragments in HeLa cells and their role in the reassembly pathway. J. Cell Biol. *109*, 463–474.

Lucocq, J.M., Pryde, J.G., Berger, E.G., and Warren, G. (1987). A mitotic form of the Golgi apparatus in HeLa cells. J. Cell Biol. *104*, 865–874.

Lupashin, V.V., Hamamoto, S., and Schekman, R.W. (1996). Biochemical requirements for the targeting and fusion of ER-derived transport vesicles with purified yeast Golgi membranes. J. Cell Biol. *132*, 277–289.

Malhotra, V., Serafini, T., Orci, L., Shepherd, J.C., and Rothman, J.E. (1989). Purification of a novel class of coated vesicles mediating biosynthetic protein transport through the Golgi stack. Cell *58*, 329–336.

McBride, H.M., Rybin, V., Murphy, C., Giner, A., Teasdale, R., and Zerial, M. (1999). Oligomeric complexes link Rab5 effectors with NSF and drive membrane fusion via interactions between EEA1 and syntaxin 13. Cell *98*, 377–386.

Misteli, T., and Warren, G. (1994). COP-coated vesicles are involved in the mitotic fragmentation of Golgi stacks in a cell-free system. J. Cell Biol. *125*, 269–282.

Mu, F.T., Callaghan, J.M., Steele-Mortimer, O., Stenmark, H., Parton, R.G., Campbell, P.L., McCluskey, J., Yeo, J.P., Tock, E.P., and Toh, B.H. (1995). EEA1, an early endosome-associated protein: EEA1 is a conserved alpha-helical peripheral membrane protein flanked by cysteine "fingers" and contains a calmodulin-binding IQ motif. J. Biol. Chem. *270*, 13503–13511.

Nakajima, H., Hirata, A., Ogawa, Y., Yonehara, T., Yoda, K., and Yamasaki, M. (1991). A cytoskeleton-related gene, uso1, is required for intracellular protein transport in *Saccharomyces cerevisiae*. J. Cell Biol. *113*, 245–260.

Nakamura, N., Lowe, M., Levine, T.P., Rabouille, C., and Warren, G. (1997). The vesicle docking protein p115 binds GM130, a cis-Golgi matrix protein, in a mitotically regulated manner. Cell *89*, 445–455.

Nakamura, N., Rabouille, C., Watson, R., Nilsson, T., Hui, N., Slusarewicz, P., Kreis, T.E., and Warren, G. (1995). Characterization of a cis-Golgi matrix protein, GM130. J. Cell Biol. *131*, 1715–1726.

Nelson, D.S., Alvarez, C., Gao, Y.S., Garcia-Mata, R., Fialkowski, E., and Sztul, E. (1998). The membrane transport factor TAP/p115 cycles between the Golgi and earlier secretory compartments and contains distinct domains required for its localization and function. J. Cell Biol. *143*, 319–331.

Oprins, A., Duden, R., Kreis, T.E., Geuze, H.J., and Slot, J.W. (1993). Beta-COP localizes mainly to the cis-Golgi side in exocrine pancreas. J. Cell Biol. *121*, 49–59.

Orci, L., Glick, B.S., and Rothman, J.E. (1986). A new type of coated vesicular carrier that appears not to contain clathrin: its possible role in protein transport within the Golgi stack. Cell *46*, 171–184.

Orci, L., Perrelet, A., and Rothman, J.E. (1998). Vesicles on strings: morphological evidence for processive transport within the Golgi stack. Proc. Natl. Acad. Sci. USA *95*, 2279–2283.

Orci, L., Stamnes, M., Ravazzola, M., Amherdt, M., Perrelet, A., Sollner, T.H., and Rothman, J.E. (1997). Bidirectional transport by distinct populations of COPI-coated vesicles. Cell *90*, 335–349.

Owen, J.D., and Schiavo, G. (1999). A handle on NSF. Nat. Cell Biol. *1*, E127–E128.

Pelham, H.R. (1998). Getting through the Golgi complex. Trends Cell Biol. *8*, 45–49.

Pepperkok, R., Lowe, M., Burke, B., and Kreis, T.E. (1998). Three distinct steps in transport of vesicular stomatitis virus glycoprotein from the ER to the cell surface in vivo with differential sensitivities to GTP gamma S. J. Cell Sci. *111*, 1877–1888.

Pepperkok, R., Scheel, J., Horstmann, H., Hauri, H.P., Griffiths, G., and Kreis, T.E. (1993). Beta-COP is essential for biosynthetic membrane transport from the endoplasmic reticulum to the Golgi complex in vivo. Cell *74*, 71–82.

Pfeffer, S.R. (1996). Transport vesicle docking: SNAREs and associates. Annu. Rev. Cell Biol. *12*, 441–461.

Pfeffer, S.R. (1999). Transport-vesicle targeting: tethers before SNAREs. Nat. Cell Biol. *1*, E17–E22.

Rothman, J.E. (1994). Mechanisms of intracellular protein transport. Nature *372*, 55–63.

Rothman, J.E., and Wieland, F.T. (1996). Protein sorting by transport vesicles. Science *272*, 227–234.

Sapperstein, S.K., Lupashin, V.V., Schmitt, H.D., and Waters, M.G. (1996). Assembly of the ER to Golgi SNARE complex requires Uso1p. J. Cell Biol. *132*, 755–767.

Sapperstein, S.K., Walter, D.M., Grosvenor, A.R., Heuser, J.E., and Waters, M.G. (1995). p115 is a general vesicular transport factor related to the yeast endoplasmic reticulum to Golgi transport factor Uso1p. Proc. Natl. Acad. Sci. USA *92*, 522–526.

Scales, S.J., Pepperkok, R., and Kreis, T.E. (1997). Visualization of ER-to-Golgi transport in living cells reveals a sequential mode of action for COPII and COPI. Cell *90*, 1137–1148.

Shima, D.T., Cabrera-Poch, N., Pepperkok, R., and Warren, G. (1998). An ordered inheritance strategy for the Golgi apparatus: visualization of mitotic disassembly reveals a role for the mitotic spindle. J. Cell Biol. *141*, 955–966.

Shima, D.T., Haldar, K., Pepperkok, R., Watson, R., and Warren, G. (1997). Partitioning of the Golgi apparatus during mitosis in living HeLa cells. J. Cell Biol. *137*, 1211–1228.

Shorter, J., and Warren, G. (1999). A role for the vesicle tethering protein, p115, in the postmitotic stacking of reassembling Golgi cisternae in a cell-free system. J. Cell Biol. *146*, 57–70.

Söllner, T., Whiteheart, S.W., Brunner, M., Erdjument-Bromage, H., Geromanos, S., Tempst, P., and Rothman, J.E. (1993). SNAP receptors implicated in vesicle targeting and fusion. Nature *362*, 318–324.

Sönnichsen, B., Lowe, M., Levine, T., Jamsa, E., Dirac-Svejstrup, B., and Warren, G. (1998). A role for giantin in docking COPI vesicles to Golgi membranes. J. Cell Biol. *140*, 1013–1021.

Sönnichsen, B., Watson, R., Clausen, H., Misteli, T., and Warren, G. (1996). Sorting by COP I-coated vesicles under interphase and mitotic conditions. J. Cell Biol. *134*, 1411–1425.

Sztul, E., Colombo, M., Stahl, P., and Samanta, R. (1993). Control of protein traffic between distinct plasma membrane domains: requirement for a novel 108,000 protein in the fusion of transcytotic vesicles with the apical plasma membrane. J. Biol. Chem. *268*, 1876–1885.

Tang, B.L., Peter, F., Krijnse-Locker, J., Low, S.H., Griffiths, G., and Hong, W. (1997). The mammalian homolog of yeast Sec13p is enriched in the intermediate compartment and is essential for protein transport from the endoplasmic reticulum to the Golgi apparatus. Mol. Cell. Biol. *17*, 256–266.

Terbush, D.R., Maurice, T., Roth, D., and Novick, P. (1996). The exocyst is a multiprotein complex required for exocytosis in *Saccharomyces cerevisiae*. EMBO J. *15*, 6483–6494.

Ungermann, C., Sato, K., and Wickner, W. (1998). Defining the functions of trans-SNARE pairs. Nature *396*, 543–548.

Warren, G. (1993). Membrane partitioning during cell division. Annu. Rev. Biochem. *62*, 323–348.

Waters, M.G., Clary, D.O., and Rothman, J.E. (1992). A novel 115-kDa peripheral membrane protein is required for intercisternal transport in the Golgi stack. J. Cell Biol. *118*, 1015–1026.

Weber, T., Zemelman, B.V., McNew, J.A., Westermann, B., Gmachl, M., Parlati, F., Sollner, T.H., and Rothman, J.E. (1998). SNAREpins: minimal machinery for membrane fusion. Cell *92*, 759–772.

Weidman, P., Roth, R., and Heuser, J. (1993). Golgi membrane dynamics imaged by freeze-etch electron microscopy: views of different membrane coatings involved in tubulation versus vesiculation. Cell *75*, 123–133.

Weis, W.I., and Scheller, R.H. (1998). Membrane fusion: SNARE the rod, coil the complex. Nature *395*, 328–329.

Yamakawa, H., Seog, D.H., Yoda, K., Yamasaki, M., and Wakabayashi, T. (1996). Uso1 protein is a dimer with two globular heads and a long coiled-coil tail. J. Struct. Biol. *116*, 356–365.